Modelling droughts and ENSO cycles in the Murray-Darling basin with a regional climate model

J.P. Evans[1]
[1]Climate Change Research Centre
The University of New South Wales
Sydney NSW 2502
AUSTRALIA

E-mail: jason.evans@unsw.edu.au

The climate of the Murray-Darling Basin (MDB) has been simulated using the Weather Research and Forecasting (WRF) model. WRF was implemented using a 10km horizontal grid and integrated for 24 years from 1985 through 2008. The model simulated climate was evaluated against gridded precipitation and temperature observations from the Australian Water Availability Project (AWAP) and found to perform adequately. WRF is able to capture the recent drought well for the basin except for an overestimation of the negative anomaly in the northernmost part of the domain. Examining ENSO cycles showed WRF has good skill at capturing the correct spatial distribution of precipitation anomalies associated with El Nino/La Nina events during this 24 year period. This high resolution simulation allows investigation of land – atmosphere coupling within the basin including identification of the dominant water vapour source regions for events and seasons, and quantification of the precipitation recycling.

1. INTRODUCTION

The Murray-Darling Basin (MDB) is Australia's "food basket" (Nicholls, 2004), accounting for 40% of Australia's agricultural production and utilizing about 70% of all water used for agriculture across the nation. The 1,500,000 hectares under irrigation for crops and pastures represents 70% of the total area under irrigation in Australia. More than 80% of the divertible surface water resource is consumed locally. Agricultural productivity within the MDB is dependent on climate and is vulnerable to climate variability and change. For example Australia's agricultural production index decreased almost 20% from the La Niña year 2001 to the El Niño year 2002 (FAOSTAT, 2005).

The MDB is one of the world's major river systems. It covers a catchment area of ~$1x10^6$ km^2 or ~14% of Australia. It contains Australia's three longest rivers; the Darling, Murray and Murrumbidgee. Unlike most other major basins of the world, the MDB is dominantly semi-arid with a very low ratio of discharge to precipitation and high interannual variability largely associated with ENSO. The MDB will continue to play a dominant role in Australia's agricultural future making improved knowledge of the hydrological impact of global warming and continued land-use change vitally important for economic development and national prosperity. Improving our understanding of the MDB's total water cycle (on land and in the atmosphere) and how this could change in the future is essential for a comprehensive assessment of impacts of human modification on the surface hydrology.

The MDB contains the largest mountain range in Australia and is significantly impacted by events in the Pacific, Indian and Southern Ocean. Due to these factors understanding of the current and future climate of the MDB is both important and difficult. A high resolution Regional Climate Model (RCM) simulation has been performed that will be used to address various climate related issues for the region. Initial evaluation of this simulation is presented here along with an evaluation of the water cycle it produces.

2. REGIONAL CLIMATE MODEL

The Weather Research and Forecasting (WRF) modelling system is developed as a collaborative partnership between the National Center for Atmospheric Research (NCAR), the National Oceanic and Atmospheric Administration (the National Centers for Environmental Prediction (NCEP) and the

Forecast Systems Laboratory (FSL)), the Air Force Weather Agency (AFWA), the Naval Research Laboratory, Oklahoma University, and the Federal Aviation Administration (FAA) in the USA as well as the wider research community. The version used in this study is the Advanced Research WRF (ARW) version 3, maintained at NCAR (Shamarock et al. 2008).

WRF was run over the Murray-Darling Basin (MDB) from 1985 through 2007, this does not include the first 2 months of the simulation that are discarded as spin-up. The model used the following physics schemes: WRF Single Moment 5-class microphysics scheme; the Rapid Radiative Transfer Model (RRTM) longwave radiation scheme; the Dudhia shortwave radiation scheme; Monin-Obukhov surface layer similarity; Noah land-surface scheme; the Yonsei University boundary layer scheme and the Kain-Fritsch cumulus physics scheme. The model simulation uses boundary conditions from the NCEP/NCAR reanalysis (NNRP) with an outer 50km resolution nest and an inner 10km resolution nest that covers the whole MDB (Figure 1). Both nests used 30 vertical levels spaced closer together in the planetary boundary layer. The NNRP is a combination of observations and a global atmosphere model, see Kalnay et al. (1996) for more information. By using as many observations as possible NNRP produces an estimate of the state of the atmosphere that is as possible to reality.

Figure 1 shows South-east Australia is dominated by large relatively flat areas. Clearly visible are the Flinders Range in South Australia and the Great Dividing Range near the east coast of Australia, with the highest peaks in the southern Snowy Mountains region. The dotted lines show a 2 degree grid which is an approximation of the resolution of Global Climate Models (GCMs). Clearly at this resolution GCMs have difficulty resolving the terrain with features such as the Flinders Range being entirely sub-grid scale and hence extremely poorly represented.

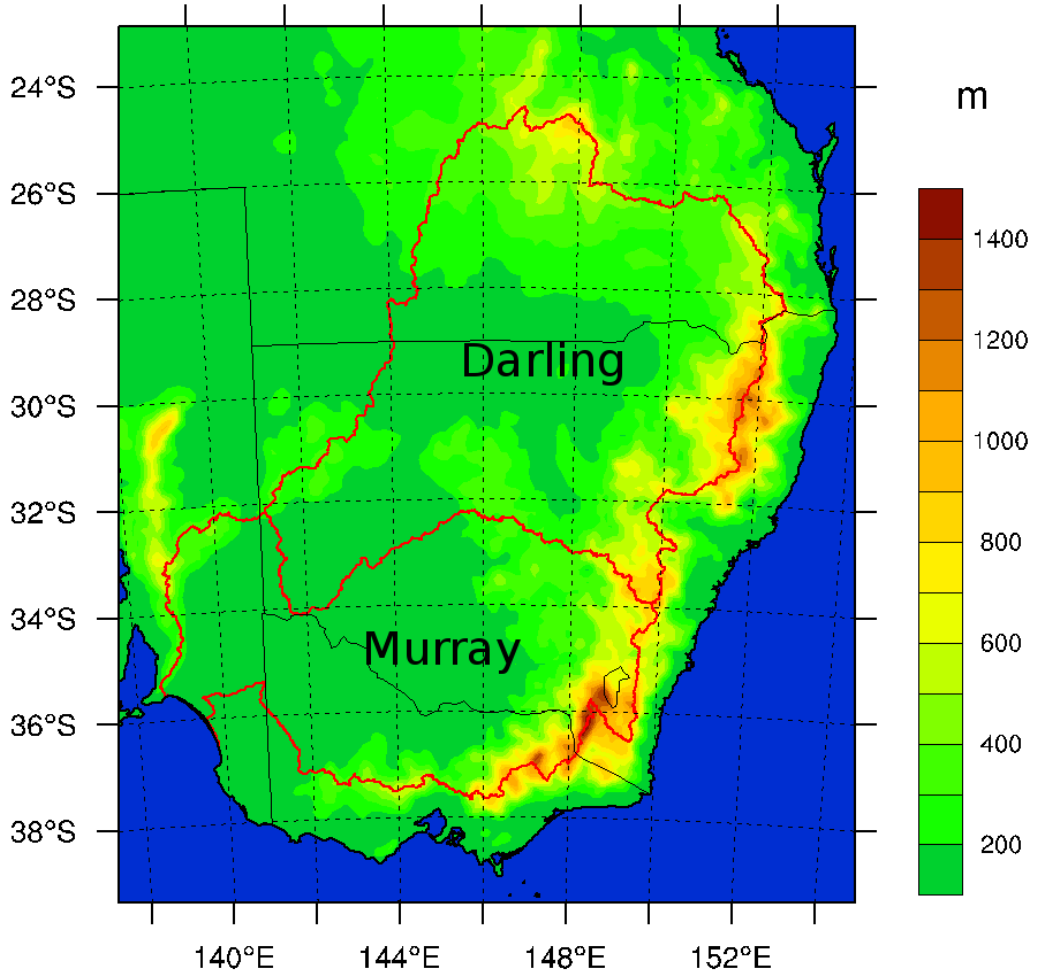

Figure 1: Regional climate model terrain (10km resolution domain)

3. OBSERVATIONS

Observations used for evaluation come from the gridded dataset prepared as part of the Australian Water Availability Project (AWAP). Details of creation of this dataset can be found in Jones et al. (2007). This dataset includes precipitation, maximum and minimum temperature, and vapour pressure surfaces obtained by interpolating surface station measurements using a three-dimensional smoothing spline onto a 0.05°x0.05° grid. The number of stations reporting varies by time and variable with precipitation interpolated from between 5,000 and 7,000 stations, while temperature fields usually have between 600 and 850 reporting stations. Solar radiation is derived from satellite measurements. Various surface hydrology parameters, such as soil moisture and runoff, are obtained using the WaterDyn hydrology model driven by the AWAP meteorological variables (Raupach et al. 2008a & b). Seasonal precipitation and mean temperature derived from the AWAP dataset for the period of interest is shown in Figure 2. The temperature increases from the high country in the South-east of the basin toward the north-west. The Murray basin has a precipitation maxima in winter and spring, while the Darling basin has a summer maxima.

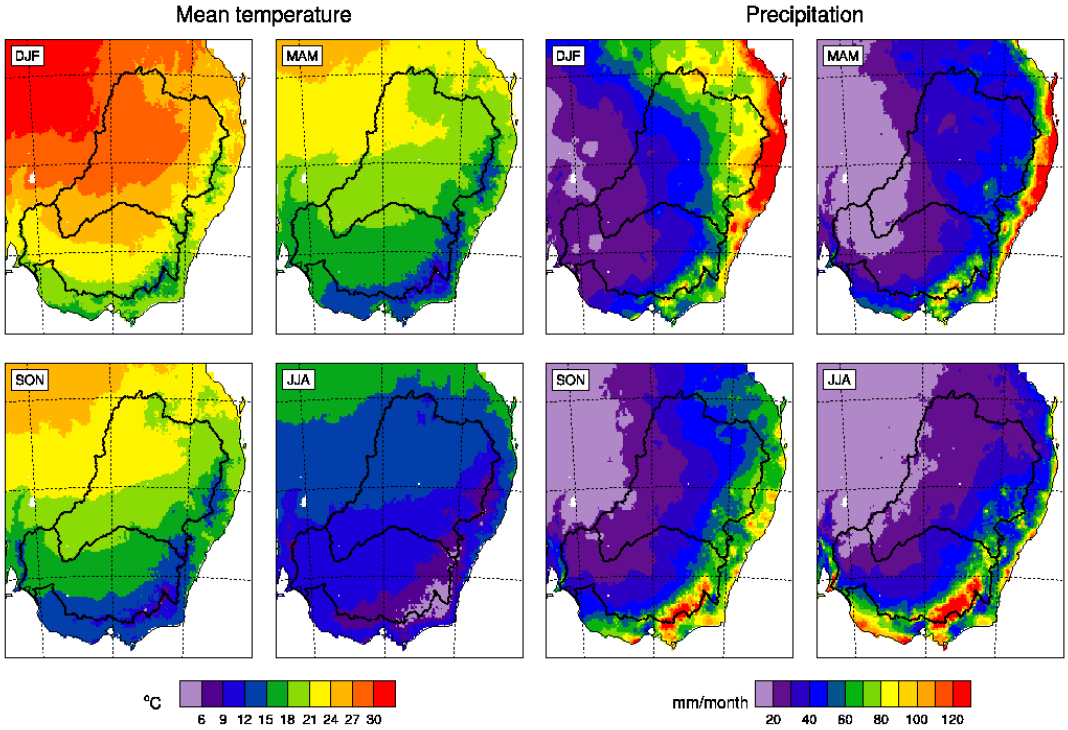

Figure 2: AWAP seasonal temperature and precipitation.

4. STATISTICAL MEASURES

Many different statistical measures have been used previously to test the performance of climate models quantitatively. Willmott, *et al.* (1985) and Legates and McCabe (1999) provide an analyses of the suitability of several of these measures as well as suggesting some of their own. In this paper the model performance is evaluated against observations using several statistics including the bias

$$Bias = \overline{M} - \overline{O} \quad (1)$$

where $\overline{M}$ is the mean of the modeled values and $\overline{O}$ is the mean of the AWAP observations. The Root Mean Square Error (RMSE) is given by

$$RMSE=\sqrt{\frac{1}{N}\sum_{i=1}^{N}\left(O_i-M_i\right)^2} \quad (2)$$

where N is the number of observed, O, and modeled, M, values being compared. Here N is the number of WRF grid cells in the domain. Climatological values are used in calculating RMSE.

In order to quantitatively evaluate the spatial agreement between model and observations, Walsh and McGregor (1997) define the pattern correlation (3), ρ_p, between observed and simulated fields simply as the correlation of a series of data points from the observed field with corresponding values from the modeled field at a fixed time, in this study monthly means are used.

$$\rho_p=\frac{\sum\left(O_i-\bar{O}\right)\left(M_i-\bar{M}\right)}{\sqrt{\sum\left(O_i-\bar{O}\right)^2}\sqrt{\sum\left(M_i-\bar{M}\right)^2}} \quad (3)$$

The anomaly correlation, ρ_a, is similar to the pattern correlation except that fields are replaced by anomalies from climatology. The anomaly correlation provides a more rigorous test of whether the model can capture the spatial pattern of interannual variations. Here the sums are calculated over the number of WRF grid cells within the domain.

5. RESULTS

In this section the results of the WRF simulations are first evaluated against the AWAP observations. Various aspects of the water cycle are then examined noting the models ability to capture drought periods and ENSO cycles.

5.1. Precipitation and Temperature

Figure 3 shows the difference in seasonal temperature between the simulations and AWAP observations. The reanalysis (NNRP) fails to capture the topography of the great dividing range and hence overestimates temperatures there while WRF is much better at capturing temperatures in that region. Also note that the NNRP generally underestimates temperatures in the north-east of the domain and this underestimation extends throughout the domain during winter. WRF generally performs better at capturing the temperatures in the north-east though it also contains a winter cold bias in the Murray basin. WRF overestimates the temperatures through much of the domain, particularly toward the north-west in Spring and Summer. This overestimation is inherited partially from the NNRP boundary conditions but WRF has increased the warm bias in these seasons compared to NNRP. These results are reflected in Table 1 where it can be seen that on an annual basis WRF overestimates temperatures in the Murray basin by 0.24K while NNRP underestimates them by overestimates temperatures in the Murray basin by 0.24K while NNRP underestimates them by 0.29K. While WRF produces only marginal improvements in pattern and anomaly correlation over NNRP it has a significantly better root mean square error (RMSE). So while WRF is able to capture the spatial temperature distribution better than NNRP, the changes in this pattern through time are only marginally closer to that found in the AWAP observations compared to NNRP. Table 2 shows a similar situation in the Darling basin though both simulation show larger biases than in the Murray basin. In the Darling basin it can also be seen that WRF produces larger improvements in the pattern and anomaly correlations suggesting it is better at capturing the time evolution of the temperature pattern here.

Figure 4 shows the seasonal precipitation differences between the simulations and the AWAP observations. It can be seen that NNRP significantly underestimates the precipitation in the high country in the south-east in all seasons while WRF produces a much better estimate of precipitation in this area, though still containing a winter underestimate. NNRP also tends to overestimate in the north-east during Summer and Autumn. WRF demonstrates a better performance in this situation however it

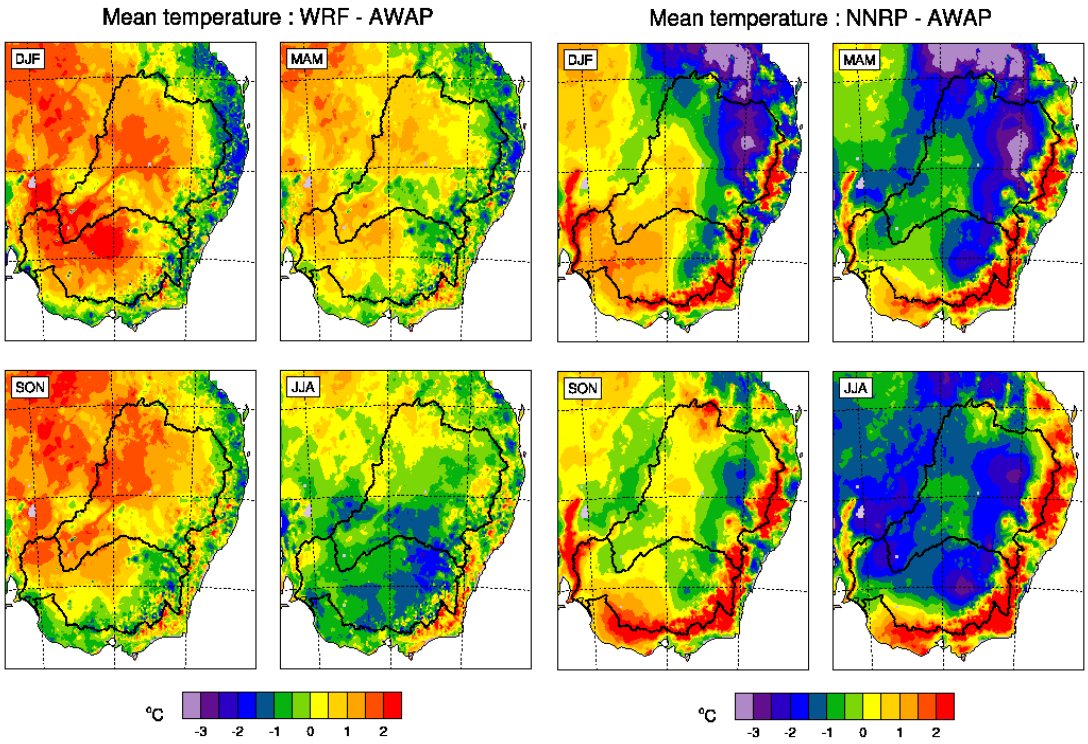

Figure 3: Difference in seasonal mean temperature (model - AWAP).

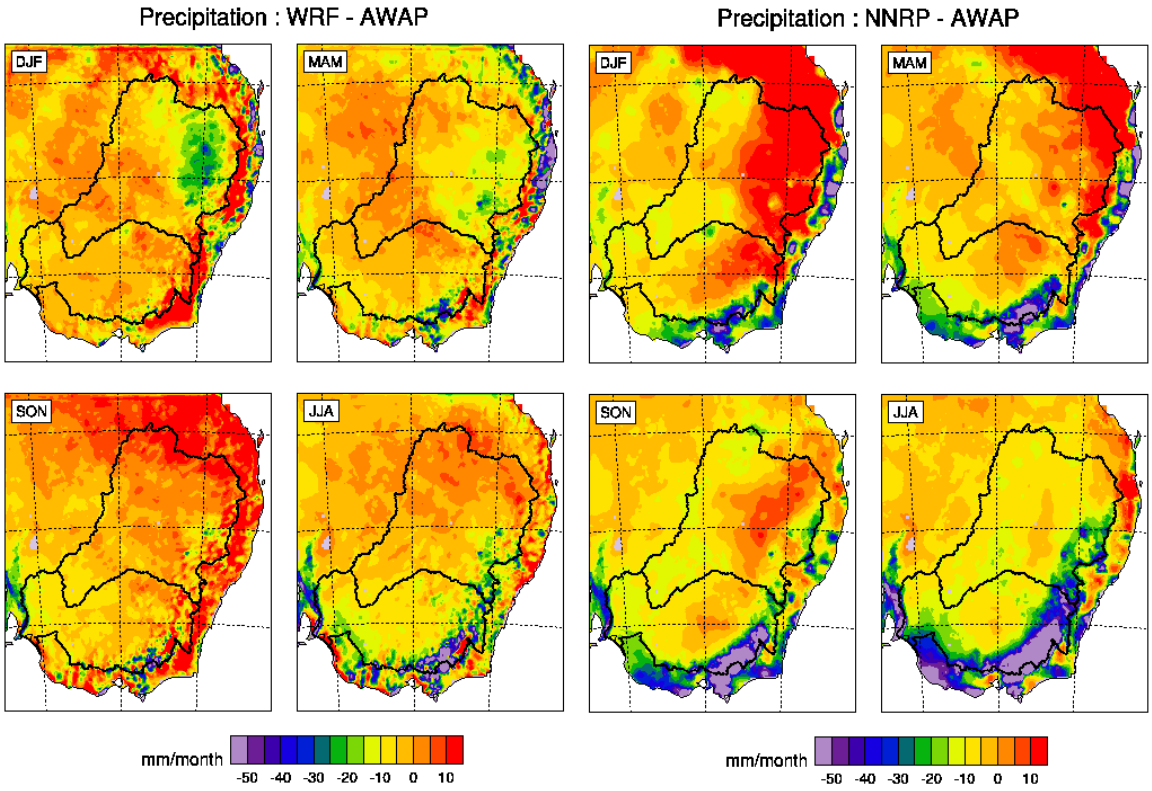

Figure 4: Difference in seasonal precipitation (model - AWAP).

Table 1: Murray River basin monthly statistics compared to AWAP. Perfect score for each statistic is given in the brackets.

	Temperature (K)		Precipitation (mm)	
	WRF	NNRP	WRF	NNRP
Bias (0)	0.72	0.21	-4.27	-13.17
RMSE (0)	0.98	1.33	9.02	20.43
Pattern Correlation (1)	0.94	0.71	0.75	0.65
Anomaly Correlation (1)	0.26	0.14	0.42	0.31

Table 2: Darling River basin monthly statistics compared to AWAP.

	Temperature (K)		Precipitation (mm)	
	WRF	NNRP	WRF	NNRP
Bias (0)	1.05	-0.62	0.04	-3.19
RMSE (0)	1.22	1.16	3.98	7.16
Pattern Correlation (1)	0.94	0.8	0.66	0.72
Anomaly Correlation (1)	0.32	0.23	0.43	0.42

tends to overestimate in this area during Spring. Table 1 shows that WRF produces improvements over NNRP in all statistics in the Murray basin. That is, the precipitation distribution produced by WRF significantly enhances that produced by it's driving model (NNRP). In the Darling basin (Table 2) the situation is less clear with mixed statistics over all. This may imply that local features such as topography are less important in the production of precipitation in the Darling basin compared to the Murray.

5.2. Recent Drought

The precipitation anomaly time series for the two basins (12 month running average) can be seen in Figure 5. The recent drought can be clearly seen with an extended period of negative anomalies extending from 2002 through to the present in both basins and in both the AWAP observations and the WRF simulation. Similar low rainfall years occurred in 1991 and 1994 in both basins, and 1997 in the Murray basin only. In each case WRF agrees quite well with the AWAP data in terms of producing below average rainfall. It is worth noting that the rainfall produced in the Murray basin for the recent drought is reproduced well by WRF but in the Darling basin WRF predicts a consistently larger negative rainfall anomaly after the initial drop in 2002.

AWAP produced both gridded datasets of meteorological observations (temperature, precipitation etc) based on station observations and using a water balance model WaterDyn, it produced gridded datasets of various components of the surface water and energy balance. In this case WaterDyn is forced using the AWAP meteorological data but the state of the land surface does not influence the local meteorology at all. WRF uses the Noah Land surface model to simulate the surface water and energy cycles. In this case the land surface is fully coupled with the atmosphere and hence feedbacks between the land surface and atmosphere are included. Figure 6 displays the soil moisture anomalies in the root zone simulated by each model. The actual depth of the soil layer used in WaterDyn various according to soil types. The mean soil depth in the Murray basin is 90cm, while in the Darling basin it is 99cm. The Noah soil moisture is always from the top metre of soil. Figure 6 shows that despite

having almost identical precipitation anomalies in the Murray basin, WaterDyn produces a larger soil moisture anomaly compared to WRF. In the Darling basin the soil moisture anomalies simulated by the two models are almost identical despite WRF having a larger precipitation anomaly.

The spatial distribution of the precipitation and soil moisture anomalies are shown in Figure 7 and Figure 8. The precipitation anomalies are distributed quite differently especially in the Darling basin with WRF having the largest anomalies near the northern and eastern boundary and AWAP having a swath across the basin with the largest anomaly. The transition from precipitation anomaly to soil moisture anomaly is quite different with WaterDyn generally producing larger soil moisture anomalies for the same precipitation anomaly. The effect of varying the soil depth in WaterDyn has alarge impact on this soil moisture anomaly distribution. The soil depth varies from 0.15m to 1.9m which translates into soil moisture holding capacities varying from ~60mm up to ~900mm. These very large differences in soil moisture capacity lead to large differences in soil moisture changes. There are very low soil moisture anomalies in areas with shallow soils such as the eastern Murray and the south-eastern Darling along with patches in the northern and north-eastern Darling. There are large soil moisture anomalies in areas with deep soils, largely through the centres of both the Murray and Darling basins. WRF uses different soil properties but the same soil depth throughout the domain so the impact of changes in soils is generally smaller than that seen in WaterDyn.

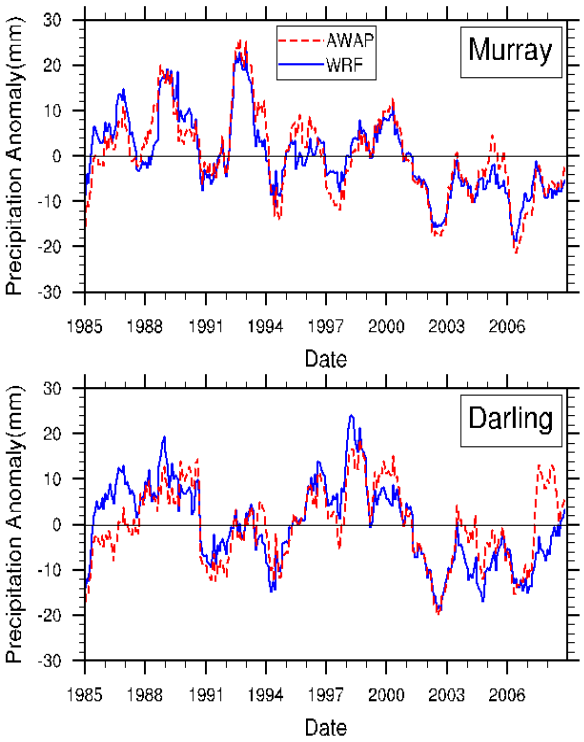

Figure 5: Precipitation anomaly time series (12 month running average) for the Murray and Darling Basins.

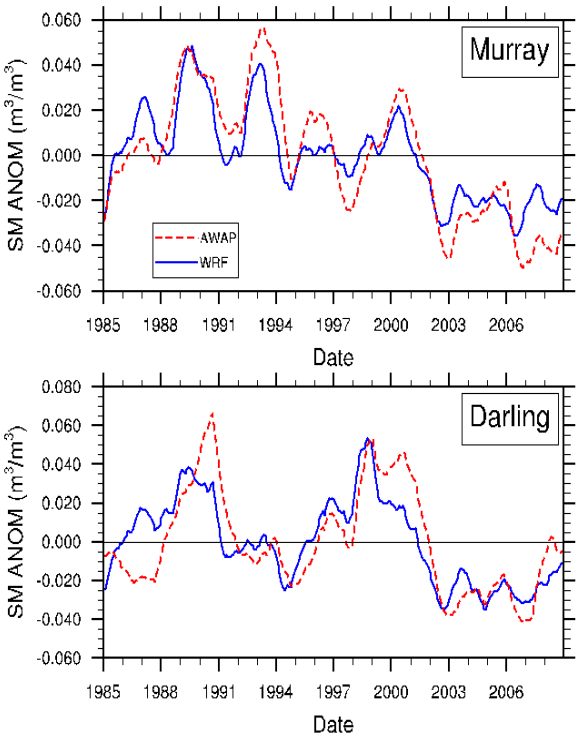

Figure 6: Root zone Soil Moisture anomaly time series (12 month running average) for the Murray and Darling basins.

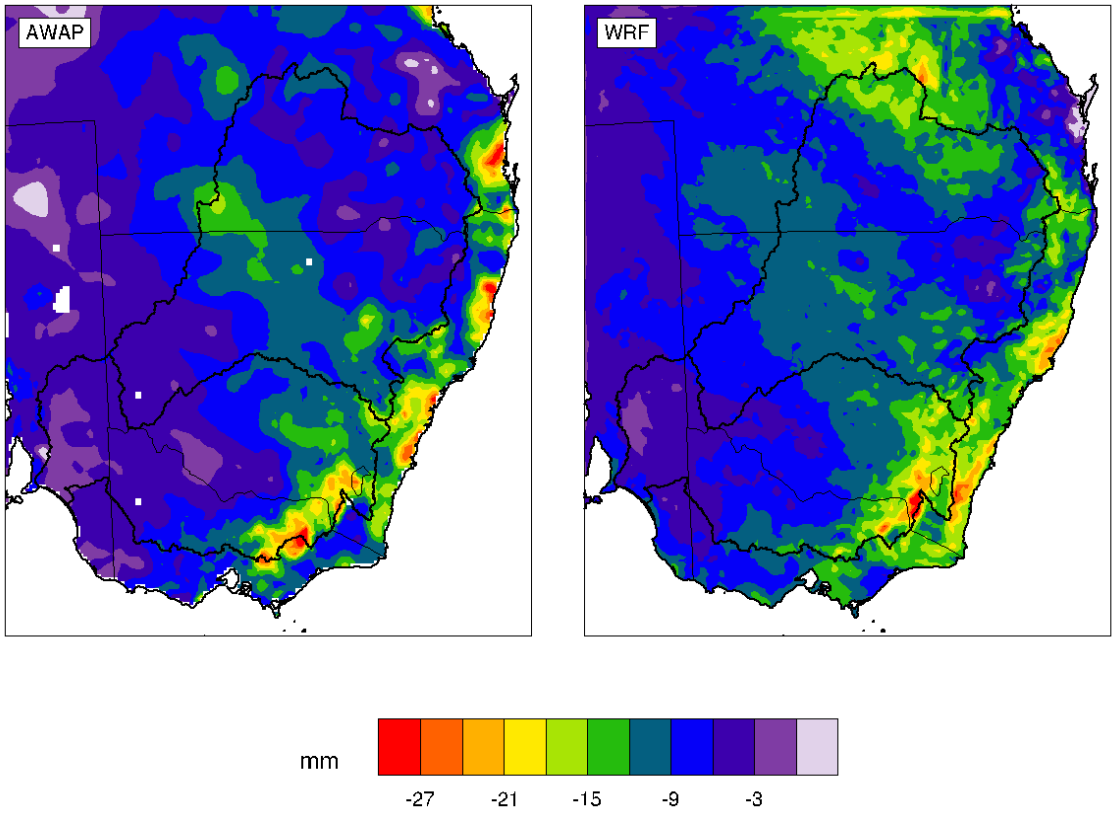

Figure 7: Precipitation anomaly: 2002-2006 minus long term mean (1985-2008).

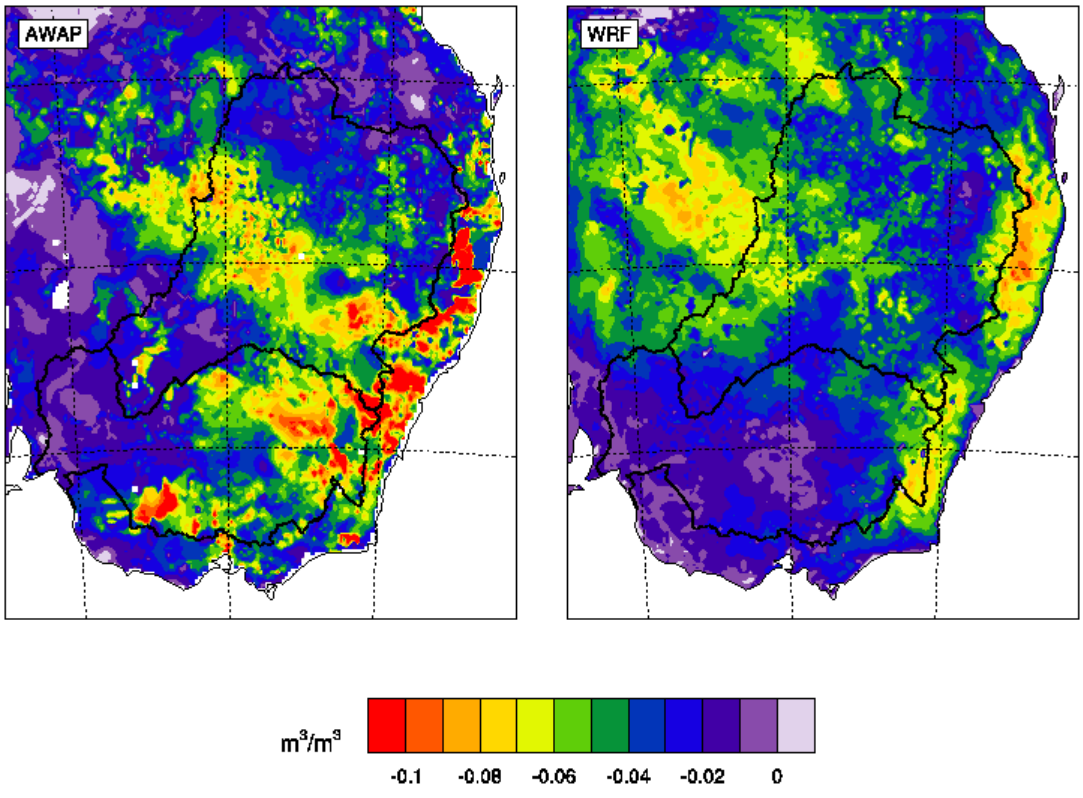

Figure 8: Soil moisture anomaly: 2002-2006 minus the long term mean (1985-2008).

5.3. ENSO cycles

Much of south-east Australian precipitation is effected by ENSO to some extent. Using the Nino 3.4 index months are defined as El Nino, neutral or La Nina. El Nino months have an index greater than 0.5, while La Nina months have an index less than -0.5. Using this definition El Nino events are spread evenly through the year (average is 10) while slightly more (less) La Nina (neutral) events occur in summer compared to winter (average is 7). Figure 9 shows the mean precipitation over all El Nino months for both AWAP and WRF. WRF is able to reproduce the general trend of a precipitation decrease across the Murray-Darling basin, with the largest decreases seen in the northern NSW coast and the NSW-Victoria coastal border and highlands region. Figure 10 Shows the equivalent figure for the La Nina precipitation anomaly. Again WRF does a good job of reproducing the anomaly associated with La Nina events with a general increase in precipitation across the Murray-Darling basin, largest in the northern Darling. It also captures the maximum increase along the Queensland-NSW coastal region and a precipitation decrease along the South Australia-Victoria coastal region.

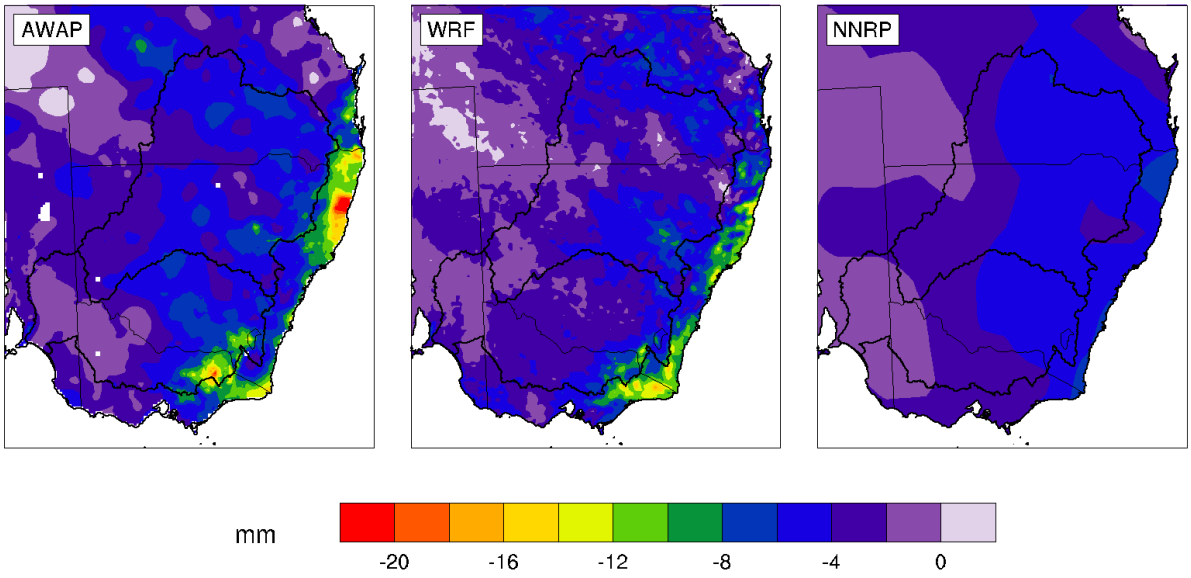

Figure 9: Precipitation anomaly during el Nino months.

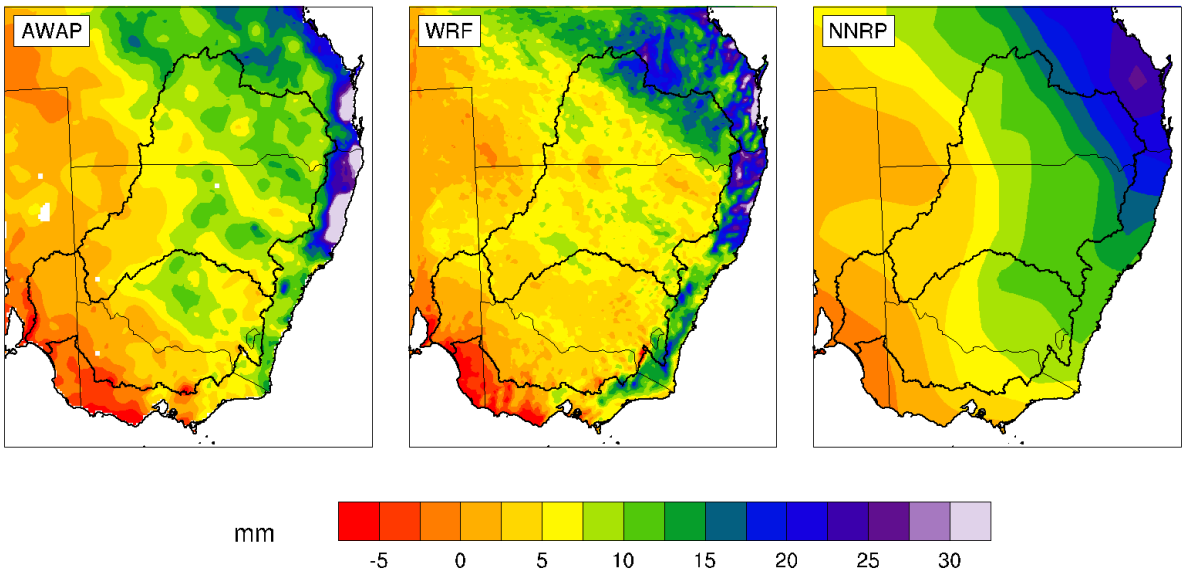

Figure 10: Precipitation anomaly during la Nina months.

6. CONCLUSIONS

The regional climate model WRF was run for 24 years over the MDB. The climate simulated by WRF was generally an improvement over that produced by the NNRP despite the fact that WRF does not assimilate any observations while NNRP does. WRF was able to reproduce the inter-annual variability reasonably well. This includes capturing the recent severe drought. While the overall magnitudes of precipitation and soil moisture anomalies were captured well the spatial distribution of these anomalies were different with WRF tending to produce larger precipitation anomalies in the northern part of the domain. When these precipitation anomalies are translated to soil moisture anomalies the differences between WaterDyn and WRF can be largely explained by the differences in the precipitation anomaly and the soil moisture depth.

WRFs ability to capture the precipitation changes associated with ENSO cycles was also evaluated. Dividing months into El Nino/neutral/La Nina based on the Nino 3.4 Index demonstrated that WRF has good skill in reproducing the spatial structure of the relevant precipitation anomalies. These results show that WRF is able to capture recent extreme events and a dominant inter-annual variation mechanism (ENSO). This high resolution simulation will facilitate investigation of land – atmosphere coupling within the basin including identification of the dominant water vapour source regions for events and seasons, and quantification of the precipitation recycling.

7. ACKNOWLEDGMENTS

This work has been funded by the Australian Research Council as part of the Discovery Project DP0772665 and the DAFF Agricultural Industries Young Innovators and Scientists Award.

8. REFERENCES

FAOSTAT data, (2005) http://faostat.fao.org/faostat/form?collection=Crops.Primary&Domain=PIN&servlet=1&hasbulk=0&version=ext&language=EN. Last accessed feb 2005.

Jones, D.A., W. Wang, R. Fawcett (2007), *Climate Data for the Australian Water Availability Project*, Final Milestone Report, Australian Bureau of Meteorology, Melbourne, Australia.

Kalnay, E., M. Kanamitsu, et al. (1996), The NCEP/NCAR 40-year reanalysis project, *Bulletin of the American Meteorological Society*, 77(3), 437-471.

Legates DR and McCabe GJ. (1999) Evaluating the use of "goodness-of-fit" measures in hydrologic and hydroclimatic model validation. Water Resources Research 35: 233-241.

Nicholls, N. (2004) The changing nature of Australian droughts, Clim. Change, 63, 323-336.

Raupach MR, PR Briggs, V Haverd, EA King, M Paget, CM Trudinger (2008a), Australian Water Availability Project (AWAP). CSIRO Marine and Atmospheric Research Component: Final Report for Phase 3.

Raupach MR, PR Briggs, V Haverd, EA King, M Paget, CM Trudinger (2008b), Australian Water Availability Project. CSIRO Marine and Atmospheric Research, Canberra, Australia. <http://www.csiro.au/awap>. 15/2/09.

Skamarock, W. C., J. B. Klemp, J. Dudhia, D.O. Gill, D.M. Barker, M.G. Duda, X.-Y. Huang, W. Wang, J.G. Powers (2008), *A Description of the Advanced Research WRF Version 3*, NCAR Technical Note, NCAR, Boulder, CO, USA.

Walsh K and McGregor J. (1997) An assessment of simulations of climate variability over Australia with a limited area model. International Journal of Climatology 17: 201-223.

Willmott CJ, Ackleson SG, Davis RE, Feddema JJ, Klink KM, Legates DR, Odonnell J and Rowe CM. (1985) Statistics for the Evaluation and Comparison of Models. Journal of Geophysical Research-Oceans 90: 8995-9005.